Simulating open quantum systems in NISQ devices with Cirq

Victor Onofre
Multiverse Computing

Mainak Roy and Jessica John Britto
Indian Institute of Technology Kharagpur

February 3rd, 2023

Concepts covered - *Open quantum systems, GLSL form of master equation, Markovian and non-Markovian dynamics, Divisibility of dynamical maps, Representation of noisy quantum channels, Quantum state tomography*

1 Introduction

In this project, we aimed to replicate some of the results presented in [put reference here] on a trapped-ion quantum computing platform using Cirq. For comparison, the original paper implements the quantum circuits in Qiskit and uses the IBM Q Experience quantum computing platform, which uses superconducting qubits.

2 Depolarizing channel

2.1 Theory

2.1.1 Pauli channel

The most general single-qubit open quantum system model is given by the time-dependent Pauli channel:

$$\frac{d\rho_s}{dt} = \frac{1}{2}\sum_i \gamma_i(t)\left[\sigma_i\rho_s(t)\sigma_i - \rho_s(t)\right]$$

where $i = x, y, z$.

The dynamics generated by the above master equation is generally not phase-covariant except if $\gamma_x(t) = \gamma_y(t)$. Also, since the decay rates may become negative, conditions for complete positivity must be imposed, which can be expressed as a set of inequalities.

The authors later use a specific form of the time dependent Pauli channel which gives rise to the phenomenon of eternal non-Markovianity: a situation where the dynamical map is non-CP-divisible for all times t. They then further use it to demonstrate a theoretical prediction, which is, the presence of oscillations in extractable work. We have not tried to replicate this result.

2.1.2 Depolarising channel

If we set $\gamma_i(t) = \gamma$ in the equation for the time-dependent Pauli channel, we get the master equation for the depolarising channel. The dynamical map of an open quantum system subject to depolarising noise is given by

$$\Phi_t\rho_s = \left[1 - \frac{3}{4}p(t)\right] + \frac{p(t)}{4}\sum_i \sigma_i\rho_s\sigma_i$$

where $i = x, y, z$ and $p(t) = 1 - e^{\gamma t}$, with γ being the Markovian decay rate.

The depolarising channel is one of the most common models of qubit decoherence because of its symmetry properties. It can be described as, with probability $1 - p$ the qubit stays the same, while with probability p it becomes maximally mixed. The mixing is described by a combination of σ_x for a bit flip error, σ_z for a phase flip error, and σ_y for both.

The authors experimentally simulate this channel for various initial states (though they only provide the plot for one specific example $|\psi\rangle = \cos\frac{\pi}{8}|0\rangle + \sin\frac{\pi}{8}e^{\frac{i\pi}{4}}|1\rangle$) and find the density matrix elements using quantum state tomography, and compare them with theoretical predictions for various values of p. They observe that the agreement between theory and experiment is independent of the intial state.

2.2 Implementation

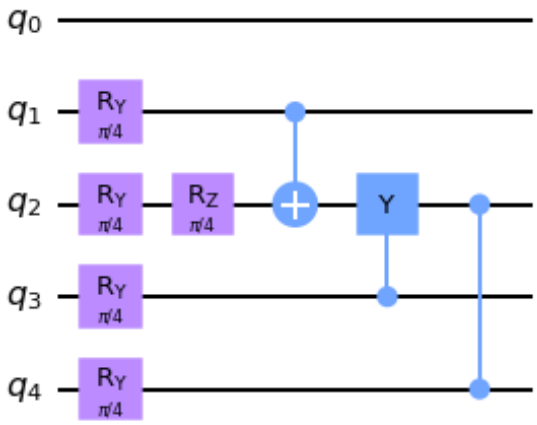

Figure 1: Circuit diagram for depolarising noise

First we prepare the system qubit in the state $|\psi\rangle = \cos\frac{\pi}{8}|0\rangle + \sin\frac{\pi}{8}e^{\frac{i\pi}{4}}|1\rangle$ using a Y rotation and a Z rotation. To get the effect of the depolarising channel, we need to apply the X, Y and Z gates with the same probability. This is achieved by applying the same Y rotation on all of the control qubits.

If the probability of applying the gates is p, the angle to rotate by is given by $\theta = \frac{1}{2}\arccos(1-2p)$. We can simulate this for $p \in [0,1]$. To get the density matrix elements, we used Cirq's in-built single qubit state tomography implementation.

2.3 Simulation

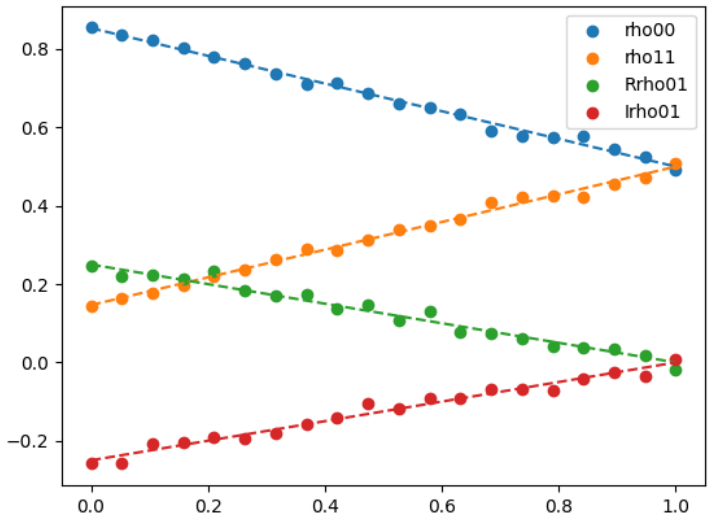

Figure 2: Simulated results for depolarising noise. The dotted lines are theoretical predictions.

The simulated results match up with what is theoretically expected.

3 Markovian reservoir engineering

3.1 Theory

Generally, the effect of the environment on a quantum system makes it lose quantum properties like coherence and entanglement. However, a carefully designed environment can give rise to interactions that drive the system to a stationary state exhibiting manifestly quantum properties.

In this example, they simulate a semigroup Markovian master equation which has the Bell state $|\psi^-\rangle = \frac{1}{\sqrt{2}}(|01\rangle - |10\rangle)$ as its stationary state.

The 4 Bell states can be identified as the eigenstates of the operators $\sigma_x^{(1)} \otimes \sigma_x^{(2)}$ and $\sigma_z^{(1)} \otimes \sigma_z^{(2)}$ as shown below:

Bell state	Eigenvalue wrt $\sigma_x^{(1)} \otimes \sigma_x^{(2)}$	Eigenvalue wrt $\sigma_z^{(1)} \otimes \sigma_z^{(2)}$
$\|\phi^+\rangle = \frac{1}{\sqrt{2}}(\|00\rangle + \|11\rangle)$	$+1$	$+1$
$\|\phi^-\rangle = \frac{1}{\sqrt{2}}(\|00\rangle - \|11\rangle)$	-1	$+1$
$\|\psi^+\rangle = \frac{1}{\sqrt{2}}(\|01\rangle + \|10\rangle)$	$+1$	-1
$\|\psi^-\rangle = \frac{1}{\sqrt{2}}(\|01\rangle - \|10\rangle)$	-1	-1

Now, they design two channels which they name the XX pump and the ZZ pump. The action of each is to pump states from the $+1$ eigenspace to the -1 eigenspace of the corresponding operator. From the table above, we can see that the only state belonging to the -1 eigenspace of both $\sigma_x^{(1)} \otimes \sigma_x^{(2)}$ and $\sigma_z^{(1)} \otimes \sigma_z^{(2)}$ is $|\psi^-\rangle$. So if we compose the two channels and apply them together, we should be able to pump everything to a single state, which is $|\psi^-\rangle$. Also, applying any one channel by itself will obviously pump states to a mixture of the states in the corresponding -1 eigenspace (which is $\{|\phi^-\rangle, |\psi^-\rangle\}$ for the XX pump and $\{|\psi^+\rangle, |\psi^-\rangle\}$ for the ZZ pump).

The forms of the XX pump and ZZ pump are given as

$$\Phi_{xx}\rho_s = E_{1x}\rho_s E_{1x}^\dagger + E_{2x}\rho_s E_{2x}^\dagger$$
$$\Phi_{zz}\rho_s = E_{1z}\rho_s E_{1z}^\dagger + E_{2z}\rho_s E_{2z}^\dagger$$

with

$$E_{1z} = \sqrt{p}\mathbb{I}^{(1)} \otimes \sigma_x^{(2)} \frac{1}{2}(\mathbb{I} + \sigma_z^{(1)} \otimes \sigma_z^{(2)})$$
$$E_{1z} = \frac{1}{2}(\mathbb{I} - \sigma_z^{(1)} \otimes \sigma_z^{(2)}) + \frac{\sqrt{1-p}}{2}(\mathbb{I} + \sigma_z^{(1)} \otimes \sigma_z^{(2)})$$

and E_{1x} and E_{2x} are the same with the replacements $\sigma_z^{(2)} \to \sigma_x^{(2)}$ and $\sigma_z^{(1)} \otimes \sigma_z^{(2)} \to \sigma_x^{(1)} \otimes \sigma_x^{(2)}$.

The above maps are parametrized by a parameter p with $0 \leq p \leq 1$. For $p \ll 1$, the repeated application of Φ_{zz} generates a master equation of Lindblad form with Lindblad/jump operator $V = \frac{1}{2}\mathbb{I}^{(1)} \otimes \sigma_z^{(2)} \left(\mathbb{I} + \sigma_z^{(1)} \otimes \sigma_z^{(2)}\right)$.

For $p = 1$, the map generates $|\psi^-\rangle$ always.

To experimentally simulate the above, the authors provide circuit implementations of each pump. Then they compare the theoretical and experimental results of applying each pump individually and their composition for different values of p.

3.2 Implementation

We'll start with some Bell state (any state can be expressed as a linear combination of Bell states, so it doesn't matter). We'll map it to a form that is easier to work with (details afterwards) and apply the pump on it. We'll then do the inverse mapping. Then we'll measure the overlap with the Bell states using a Bell measurement circuit. We can combine and remove CNOTs and Hadamards in these subcircuits giving the final circuit diagram for each pump.

Here's how the mapping works. Given a Bell state, we can map it to a factorised state where one qubit is an eigenstate of σ_z and the other is an eigenstate of σ_x by applying a CNOT between them. Applying the CNOT on the first system qubit with the second one as control gives us the following conversion table.

Bell state	Mapped state
$\|\phi^+\rangle = \frac{1}{\sqrt{2}}(\|00\rangle + \|11\rangle)$	$\|0\rangle\|+\rangle$
$\|\phi^-\rangle = \frac{1}{\sqrt{2}}(\|00\rangle - \|11\rangle)$	$\|0\rangle\|-\rangle$
$\|\psi^+\rangle = \frac{1}{\sqrt{2}}(\|01\rangle + \|10\rangle)$	$\|1\rangle\|+\rangle$
$\|\psi^-\rangle = \frac{1}{\sqrt{2}}(\|01\rangle - \|10\rangle)$	$\|1\rangle\|-\rangle$

Notice how we can now clearly tell which states need to be pumped. We'll use this to our advantage. Let's start by considering the ZZ pump.

3.2.1 ZZ pump

On operating the ZZ pump on the two qubits, we want the populations of $|\psi^+\rangle$ and $|\psi^-\rangle$ to increase since they belong to the -1 eigenspace of the $\sigma_z^{(1)} \otimes \sigma_z^{(2)}$ operator.

The pump works by applying an X rotation on the qubit which is an eigenstate of the σ_z operator. If the initial Bell state belonged to the $+1$ eigenspace, we will flip the state to the -1 eigenspace with some probability p (the parameter mentioned before). Working out the equation gives us the

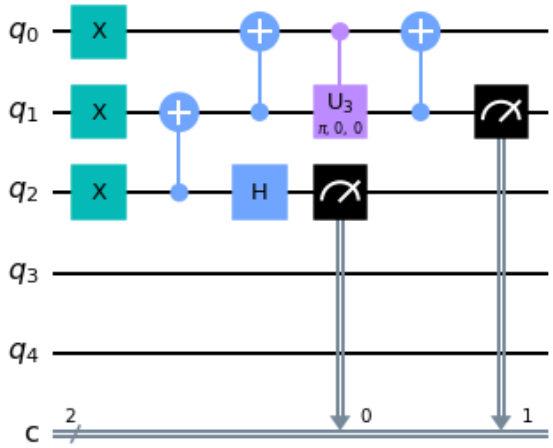

Figure 3: Circuit diagram for ZZ pump

angle of rotation $\theta = \arccos(1 - 2p)$. If the initial Bell state belonged to the -1 eigenspace, we will leave it as it is.

The simplest way to do that is to initialise an enviroment qubit to $|1\rangle$, then apply a CNOT on it controlled by the relevant system qubit, and then apply the pumping X rotation controlled by the environment qubit. If the qubit was $|1\rangle$, then the system qubit will become $|0\rangle$ and the pump will not be activated, and vice versa. After we're done, we can simply apply all the gates again in reverse to undo the mapping and bring it back to a superposition of Bell states.

Then we can measure the overlap with Bell states using a Bell measurement circuit.

3.2.2 XX pump

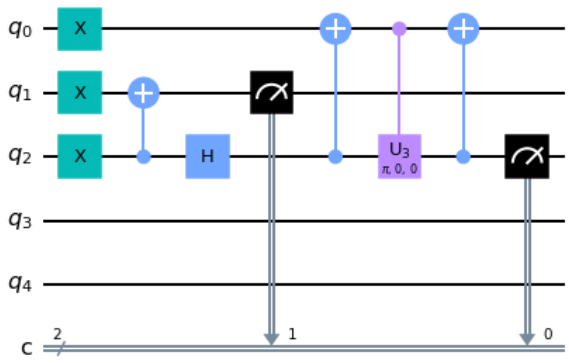

Figure 4: Circuit diagram for XX pump

On operating the XX pump on the two qubits, we want the populations of $|\psi^-\rangle$ and $|\phi^-\rangle$ to increase since they belong to the -1 eigenspace of the $\sigma_x^{(1)} \otimes \sigma_x^{(2)}$ operator.

The XX pump follows the same principles as the ZZ pump, but we are dealing with $|+\rangle$ and $|-\rangle$ here instead of $|0\rangle$ and $|1\rangle$. So we first apply a Hadamard gate and then we can do the same thing as before.

3.2.3 ZZ-XX pump

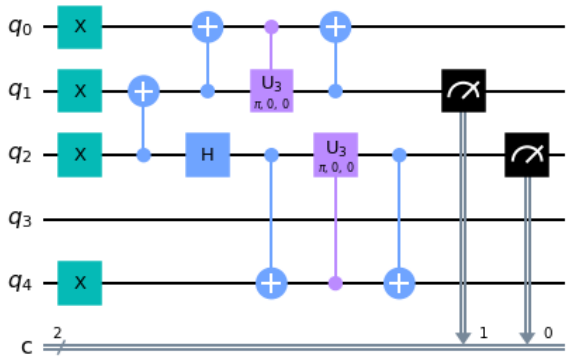

Figure 5: Circuit diagram for ZZ-XX pump

We will concatenate the ZZ and XX pumps and remove the final CNOT of the ZZ pump and the first CNOT of the XX pump.

3.3 Simulation

3.3.1 ZZ pump

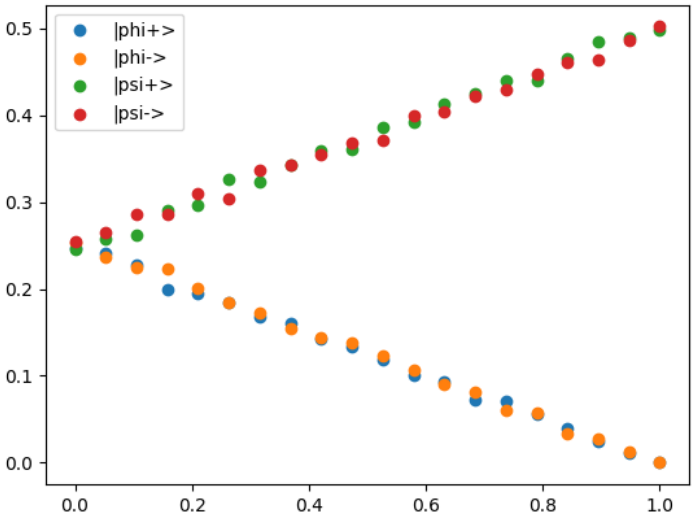

Figure 6: Simulated results for ZZ pump.

The population of states $|\psi^+\rangle$ and $|\psi^-\rangle$ are clearly increasing with increasing p.

3.3.2 XX pump

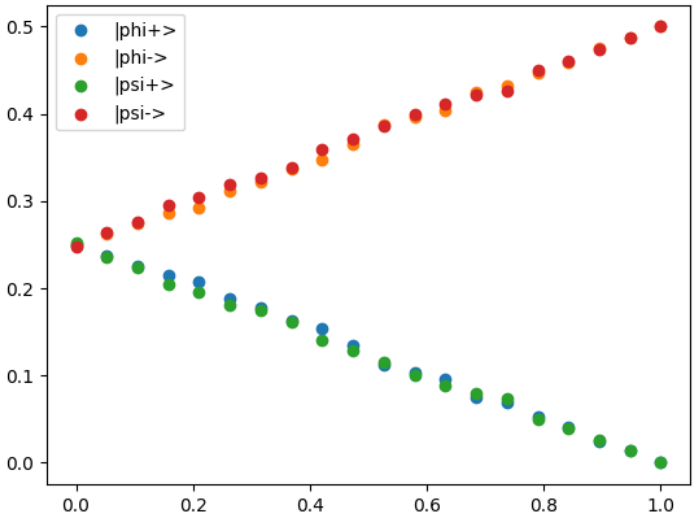

Figure 7: Simulated results for XX pump.

The population of states $|\phi^-\rangle$ and $|\psi^-\rangle$ are clearly increasing with increasing p.

3.3.3 ZZ-XX pump

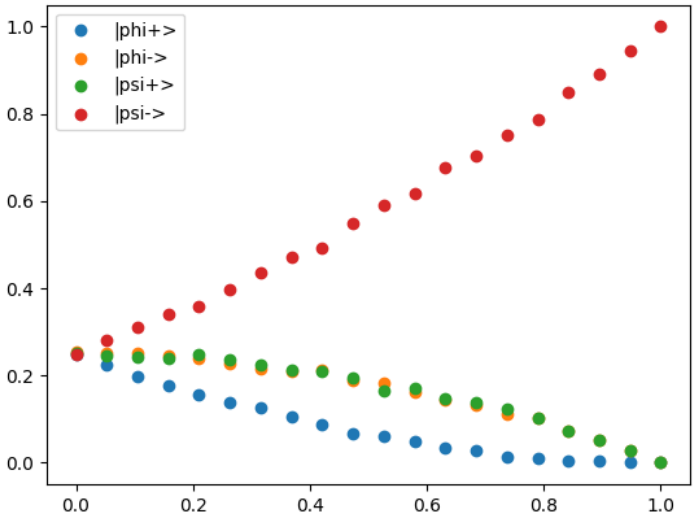

Figure 8: Simulated results for ZZ-XX pump.

The population of state $|\psi^-\rangle$ is very quickly increasing with increasing p. The populations of states $|\psi^+\rangle$ and $|\phi^-\rangle$ are decreasing, but slowly, because their populations are increased by one pump and decreased by the other. The population of state $|\phi^+\rangle$ decreases the fastest because its population is decreased by both pumps.

4 Collisional model

4.1 Theory

In this model, we take a system qubit, and repeatedly "collide" it with successive environment qubits. A collision consists of applying the unitary operator $U = e^{ig\tau\sigma_z} \otimes |0\rangle_k \langle 0| + e^{-ig\tau\sigma_z} \otimes |1\rangle_k \langle 1|$ between the system qubit and the k^{th} environmental qubit. Here, g is the coupling strength and τ is the time duration over which one collision takes place. Let us say n collisions happen in the time $t = n\tau$.

Now we consider two cases. In one case, the environment qubits are prepared in the classically correlated state $\rho = \frac{1}{2}(|0\rangle^{\otimes n} \langle 0|^{\otimes n} + |1\rangle^{\otimes n} \langle 1|^{\otimes n})$.

In the other case, the environment qubits are prepared in the uncorrelated state $|+\rangle^{\otimes n}$.

4.1.1 Correlated case

The dynamical map after n collisions is given by

$$\Phi_t\rho_S = Tr_E[U_n \cdots U_2 U_1(\rho_S \otimes \rho_{corr})U_1^\dagger U_2^\dagger \cdots U_n^\dagger] = \cos^2(ng\tau)\rho_S + \sin^2(ng\tau)\sigma_z\rho_S\sigma_z$$

If we consider $\rho_S = a\,|0\rangle\langle 0| + b\,|0\rangle\langle 1| + c\,|1\rangle\langle 0| + d\,|1\rangle\langle 1|$ (since there is only one system qubit), then applying the dynamical map above gives us

$$\Phi_t\rho_S = a\,|0\rangle\langle 0| + (\cos^2(ng\tau) - \sin^2(ng\tau))b\,|0\rangle\langle 1| + (\cos^2(ng\tau) - \sin^2(ng\tau))c\,|1\rangle\langle 0| + d\,|1\rangle\langle 1|$$

So it only affects the coherences, and it multiplies the same factor to both. So we only need to check ρ_{12} in order to quantify the effect of the dynamical map.

The map alternates intervals of Markovian and non-Markovian dynamics with a period of $\frac{\pi}{2}$. It is P-divisible in the interval $\left(0 < ng\tau < \frac{\pi}{4}\right)$ and not P-divisible in the interval $\left(\frac{\pi}{4} < ng\tau < \frac{\pi}{2}\right)$, and it repeats the pattern. When a map is not P-divisible, it is called essentially non-Markovian. We will demonstrate this non-Markovianity in the experiment.

4.1.2 Uncorrelated case

The dynamical map after n collisions is given by

$$\Phi_t\rho_S = \frac{1}{2}(1 + \cos^n(2g\tau))\rho_S + \frac{1}{2}(1 - \cos^n(2g\tau))\sigma_z\rho_S\sigma_z$$

Like before, considering $\rho_S = a\,|0\rangle\langle 0| + b\,|0\rangle\langle 1| + c\,|1\rangle\langle 0| + d\,|1\rangle\langle 1|$ gives us

$$\Phi_t\rho_S = a\,|0\rangle\langle 0| + \cos^n(2g\tau)b\,|0\rangle\langle 1| + \cos^n(2g\tau)c\,|1\rangle\langle 0| + d\,|1\rangle\langle 1|$$

The form of the result is the same as before, so the same conclusions follow. In this case, when $g\tau < \frac{\pi}{4}$ (weak coupling regime), the map gives Markovian dynamics.

4.2 Implementation

We'll take our system qubit to be in the state $\rho_S = |+\rangle$. So $a = b = c = d = \frac{1}{2}$. Note that the coefficients of the result in both cases are all real. So while density matrix elements can be complex in general, in this case it is enough to only get the real part of ρ_{12}.

The general structure of each circuit is similar. First, the system qubit is initialised to $|+\rangle$ using a Hadamard gate. Then we prepare the environment qubits. Then a series of i collisions follow where $i \in [1, c]$. For our experiment, we took $c = 7$. Finally, we apply a Hadamard gate on the system qubit. This affects the density matrix as follows:

$$H\rho_S H^\dagger = \frac{1}{\sqrt{2}}\begin{bmatrix}1 & 1\\ 1 & -1\end{bmatrix}\begin{bmatrix}\frac{1}{2} & \frac{x}{2}\\ \frac{x}{2} & -\frac{1}{2}\end{bmatrix}\frac{1}{\sqrt{2}}\begin{bmatrix}1 & 1\\ 1 & -1\end{bmatrix} = \begin{bmatrix}\frac{1+x}{2} & 0\\ 0 & \frac{1-x}{2}\end{bmatrix}$$

So we can then measure the populations of $|0\rangle$ and $|1\rangle$, subtract them, and then divide by number of shots to find out x (where x is the factor the coherences are multiplied by in each case). Then we know that $\rho_{12} = \frac{x}{2}$.

A collision is performed in the following way. We apply a CNOT gate on the system qubit controlled by the relevant environment qubit, then apply a Z rotation by the required factor, then apply the same CNOT again. If we work it out, we'll find that it reproduces the unitary U.

4.2.1 Correlated case

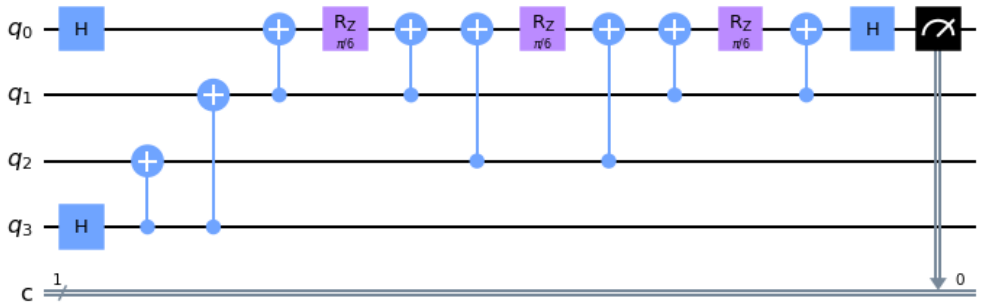

Figure 9: Circuit diagram for 3 collisions in the correlated case.

We can greatly reduce our qubit usage in the correlated case. A naive implementation of the circuit might take n qubits, but we can actually do it with just 3 qubits.

When we are doing a collision, we are working with the reduced density matrix of one environment qubit. Working out the effect of U on the reduced density matrix of the system qubit and the environment qubit in this case (which is $|+\rangle\langle+| \otimes \frac{I}{2}$, i.e. the environment qubit is maximally mixed) shows that it leaves the reduced density matrix of the environment qubit invariant. Effectively, what this means is that we can collide with any qubit in any order since the density matrix of environment qubits stays the same under the action of U.

Next, we shouldn't collide with the same qubit twice in a row. The reason is that the compiler would optimise the circuit and remove the second CNOT of the first collision and the first CNOT of the second collision and create a combined rotation, which we don't want. This means we should have at least 2 qubits to collide with.

For the form of the density matrix of the environment qubits in this case, we can note that when we trace out all qubits except one to get its reduced density matrix, the final result is independent of n. So all we really require is $n = 2$ for the reasons discussed above.

To get that density matrix, we can first prepare 3 qubits in the GHZ state $\psi_{GHZ} = \frac{|000\rangle+|111\rangle}{\sqrt{2}}$, and then we can trace out any one of the qubits to give us the required density matrix, which is the reduced density matrix of the remaining two qubits. We'll collide with these two qubits alternately.

4.2.2 Uncorrelated case

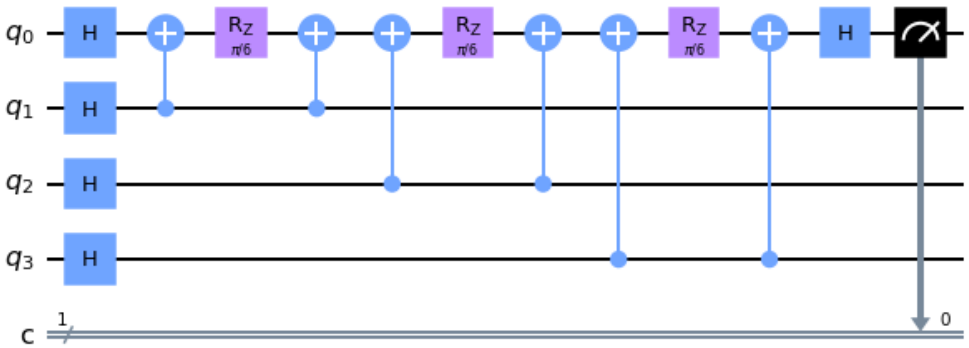

Figure 10: Circuit diagram for 3 collisions in the uncorrelated case.

In this case, we simply apply a Hadamard gate on each environment qubit to get them to the state $|+\rangle^{\otimes n}$. Then we perform collisions with each

of the environment qubits sequentially. We can't apply the same kind of optimization as in the correlated case here because the action of U does change the reduced density matrix of the environment qubit.

4.3 Simulation

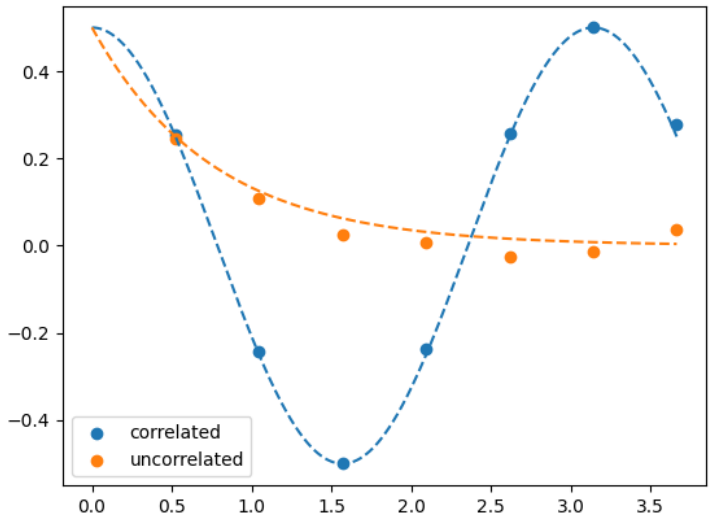

Figure 11: Simulated results for collisional model. The correlated case clearly shows oscillations in the coherences indicating non-Markovian behaviour.

The simulated results match up with what is theoretically predicted.

5 Noise model

We planned to use the Amazon Braket us-east-1 IonQ quantum computer. To get an idea of what it would look like, we created a noise model for the device in Qiskit and simulated it.

Device parameter	Value
1 qubit gate fidelity	0.9981
2 qubit gate fidelity	0.9773
SPAM fidelity	0.99752
T1 timing	10000
T2 timing	0.2
1 qubit gate timing	0.00001
2 qubit gate timing	0.0002
Readout timing	0.00013
Reset timing	0.00002

Calibration results for the IonQ device. All timings are in seconds.

The error due to thermal relaxation was negligible as compared to the error from 1 and 2 qubit gate fidelity, which was modeled by applying depolarising noise.

6 Analysis

6.1 Markovian Reservoir Engineering

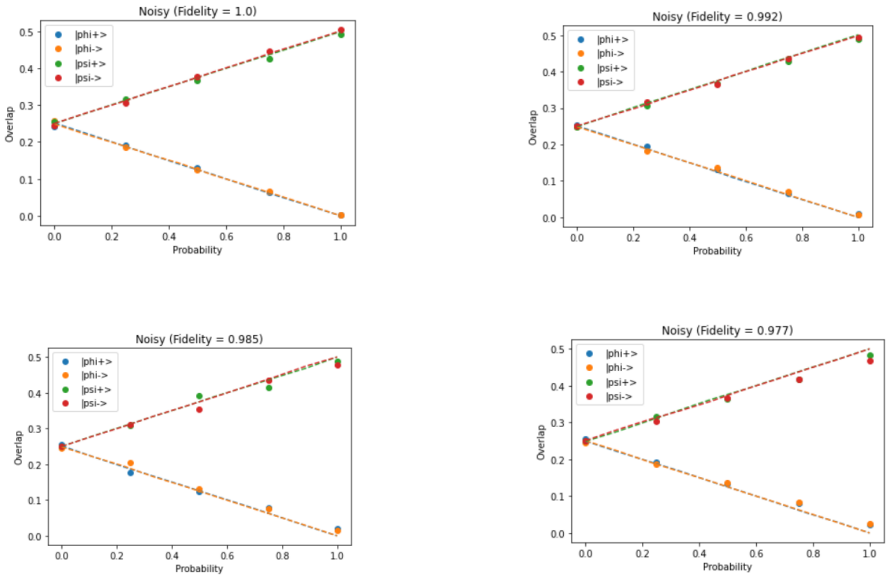

Figure 12: The dotted curves are theoretical values.

The analysis for the Markovian Reservoir Engineering is done for the case

of ZZ Pump. There is a slight dependence on two-qubit gate fidelity. This is because the circuit implementation for the ZZ pump requires 3 CNOT gates. Hence, by varying the two-qubit gate fidelity, there is not much change in the error introduced into the system.

The theoretical values were obtained for the ZZ Pump by running the circuit with a high number of shots (= 32768 shots). And also, the number of shots for finding the simulated values is 1024 shots.

We plotted the absolute error vs the parameter p for the $|\psi^+\rangle$ state (using 32768 shots this time for the simulated values).

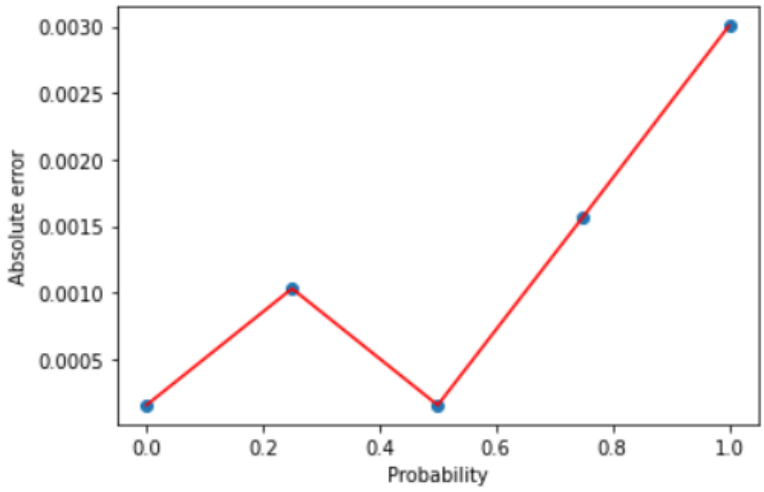

Figure 13: The absolute error seems to increase as the parameter p increases.

We tried to apply error mitigation using Zero-Noise Extrapolation in Mitiq, but as of version 0.25.0, Mitiq does not support circuits with classical flow control, so we could not apply it. It can still be done, but for now we opted not to do it because of the time and effort required.

6.2 Collisional Model

6.2.1 Correlated Case

By varying fidelity associated with the two-qubit gates, we get the following results for 256 shots and 20 collisions -

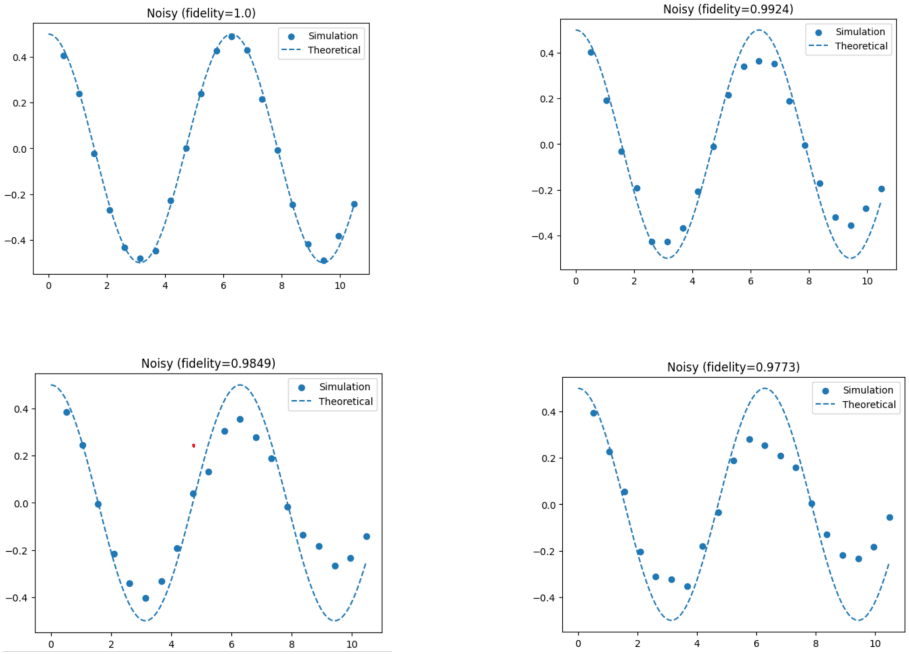

Clearly, we could see that with a decrease in fidelity, the results deviate from the theoretical curve, such that the system undergoes damping. The region surrounding the maximas and minimas have maximum deviation from the theoretical results.

We have applied **Quantum Error Mitigation** using Zero-Noise Extrapolation Technique. The extrapolation method we have used here is the **LinearFactory** Extrapolation with a linear fit with scale factors [1.0, 2.0, 3.0]. We have scaled the noise using the **fold_global** method, which performs the transformation $G \rightarrow GG^{\dagger}G$ where G is some gate. Comparison of the results for the mitigated and unmitigated cases is shown in the plot below.

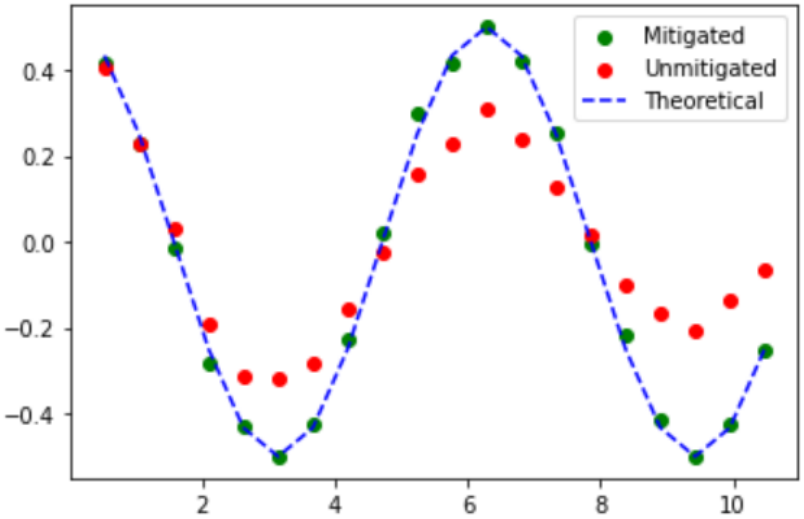

Figure 15: Simulated results for collisional model. For mitigated and unmitigated cases.

We have also plotted absolute error vs number of CNOT gates, Gate Depth vs number of CNOT gates, and mean error vs number of shots-

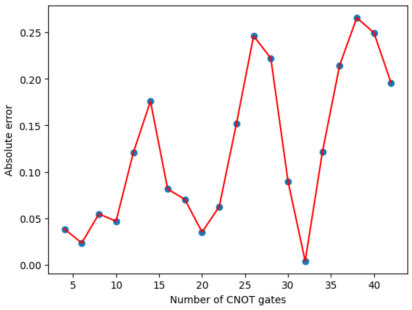

(a) The absolute error is minimum where the slope of the function is highest, and maximum at peaks.

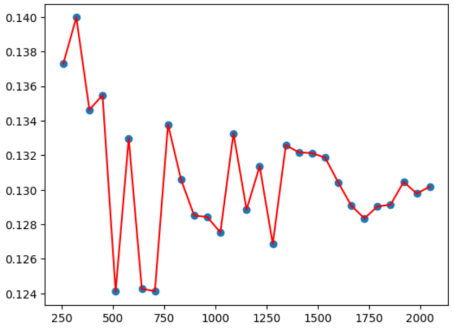

(b) The mean error eventually converges to a constant value determined by the rate of damping and the number of collisions, since the error due to random fluctuations dies out.

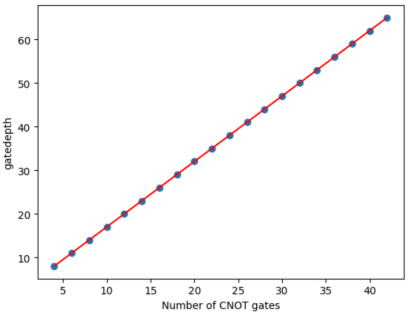

(c) A reference for how quickly the depth of the circuit increases with the number of collisions.

Figure 16: Analysis of results for correlated case

6.2.2 Uncorrelated case

By varying fidelity associated with the two-qubit gates, we get the following results for 1024 shots and 7 collisions -

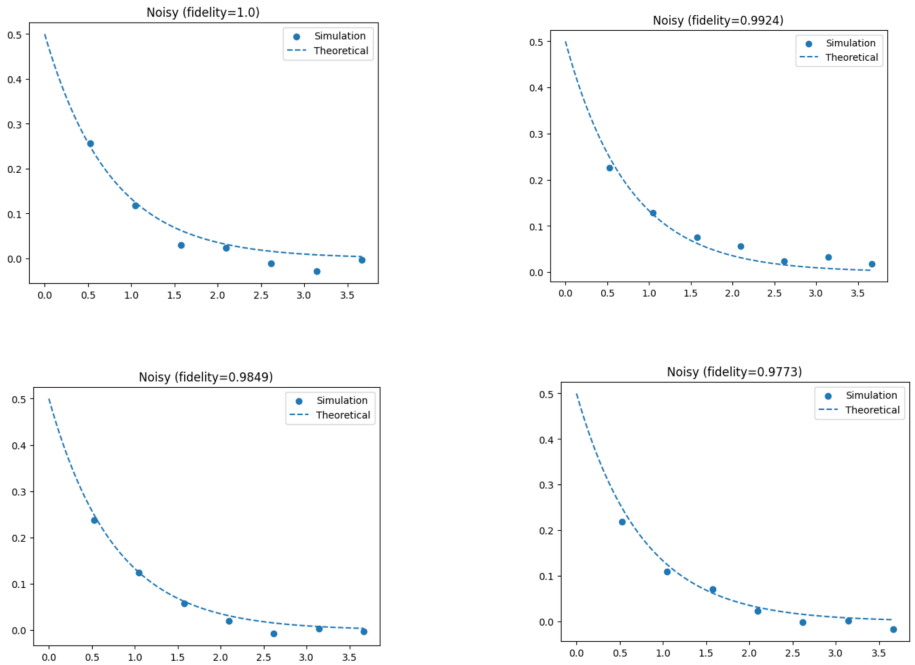

In this case, the results are not that affected by the change in fidelity.

We have also plotted absolute error vs number of CNOT gates and mean error vs number of shots (the gate depth increases at the same rate for correlated case)-

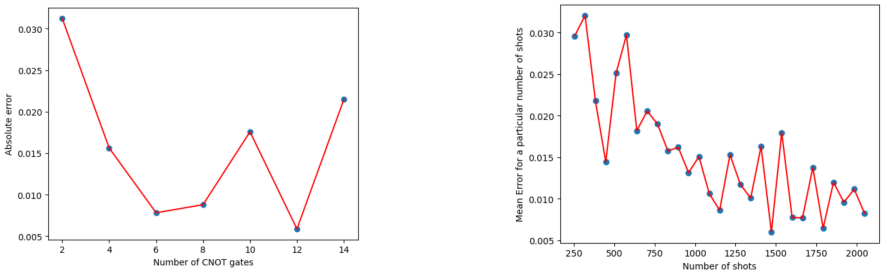

(a) The absolute error does not show any clear trend.

(b) The mean error appears to tend to zero as the number of shots increases.

Figure 18: Analysis of results for uncorrelated case

6.3 Depolarising

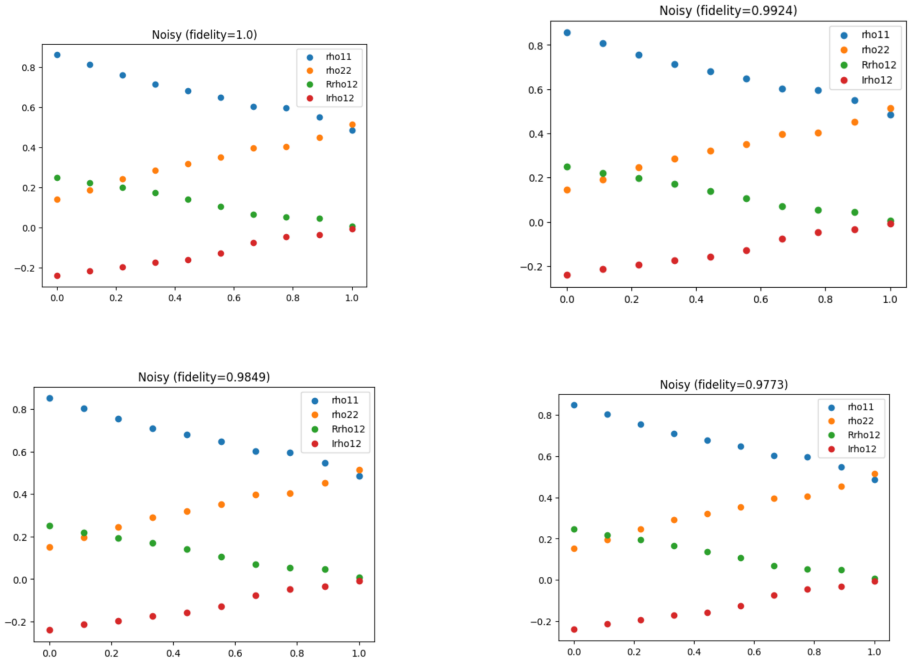

From the above plots, we can infer the effects of noise by varying the fidelity in the two-qubit gates, i.e, CNOT gates are quite negligible. This could be attributed to the fact that the circuit implementation for depolarizing requires less number of CNOT gates compared to the Collisional Model. Besides, the Depolarizing Model has a simple circuit implementation. Hence, by varying the fidelity, there is not much error introduced into the system. thereby results for the varied fidelity cases only slightly deviate from the noiseless settings.

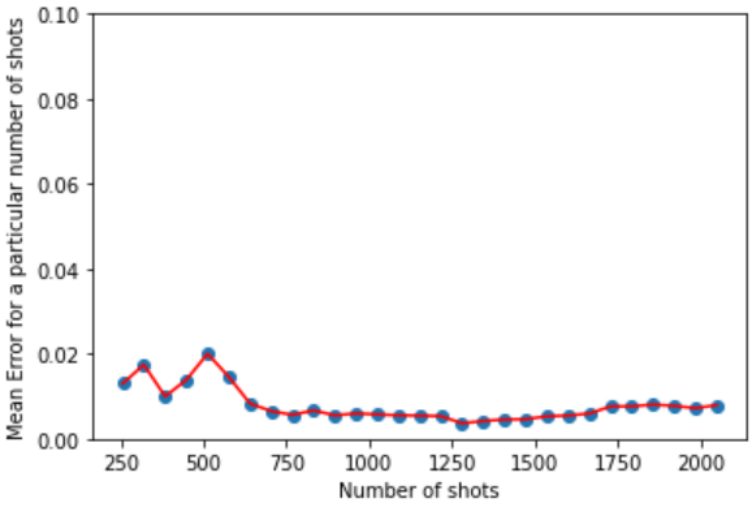

From the plot above, we can infer that the mean error in the real part of ρ_{12} is negligible after 1000 shots.

7 References

1. IBM Q Experience as a versatile experimental testbed for simulating open quantum systems
2. Quantum Error Correction: An Introductory Guide
3. Nielson and Chuang
4. Spring School on Quantum Error Correction
5. Chapter 4 from "Introduction to Classical and Quantum Computing"
6. Mitiq